

## ***Fine-scale planktonic habitat partitioning at a shelf-slope front revealed by a high-resolution imaging system***

The Faculty of Oregon State University has made this article openly available.  
Please share how this access benefits you. Your story matters.

<b>Citation</b>	Greer, A. T., Cowen, R. K., Guigand, C. M., & Hare, J. A. (2015). Fine-scale planktonic habitat partitioning at a shelf-slope front revealed by a high-resolution imaging system. <i>Journal of Marine Systems</i> , 142, 111-125. doi:10.1016/j.jmarsys.2014.10.008
<b>DOI</b>	10.1016/j.jmarsys.2014.10.008
<b>Publisher</b>	Elsevier
<b>Version</b>	Version of Record
<b>Terms of Use</b>	<a href="http://cdss.library.oregonstate.edu/sa-termsfuse">http://cdss.library.oregonstate.edu/sa-termsfuse</a>



# Fine-scale planktonic habitat partitioning at a shelf-slope front revealed by a high-resolution imaging system



Adam T. Greer <sup>a,\*</sup>, Robert K. Cowen <sup>b</sup>, Cedric M. Guigand <sup>c</sup>, Jonathan A. Hare <sup>d</sup>

<sup>a</sup> College of Engineering, University of Georgia, Boyd Graduate Studies 708A, 200 D.W. Brooks Drive, Athens, GA 30602, United States

<sup>b</sup> Hatfield Marine Science Center, Oregon State University, 2030 SE Marine Science Drive, Newport, OR 97365, United States

<sup>c</sup> Rosenstiel School of Marine and Atmospheric Science, 4600 Rickenbacker Cswy, Miami, FL 33149, United States

<sup>d</sup> Northeast Fisheries Science Center, National Marine Fisheries Service, Narragansett Laboratory, 28 Tarzwell Drive, Narragansett, RI 02882, United States

## ARTICLE INFO

### Article history:

Received 10 June 2014

Received in revised form 30 September 2014

Accepted 22 October 2014

Available online 29 October 2014

### Keywords:

Shelf edge

Fronts

Zooplankton

Larval fishes

Predator–prey

Georges Bank

Diatom aggregates

salps

gelatinous

## ABSTRACT

Ocean fronts represent productive regions of the ocean, but predator–prey interactions within these features are poorly understood partially due to the coarse-scale and biases of net-based sampling methods. We used the *In Situ* Ichthyoplankton Imaging System (ISIS) to sample across a front near the Georges Bank shelf edge on two separate sampling days in August 2010. Salinity characterized the transition from shelf to slope water, with isopycnals sloping vertically, seaward, and shoaling at the thermocline. A frontal feature defined by the convergence of isopycnals and a surface temperature gradient was sampled inshore of the shallowest zone of the shelf-slope front. Zooplankton and larval fishes were abundant on the shelf side of the front and displayed taxon-dependent depth distributions but were rare in the slope waters. Supervised automated particle counting showed small particles with high solidity, verified to be zooplankton (copepods and appendicularians), aggregating near surface above the front. Salps were most abundant in zones of intermediate chlorophyll-*a* fluorescence, distinctly separate from high abundances of other grazers and found almost exclusively in colonial form (97.5%). Distributions of gelatinous zooplankton differed among taxa but tended to follow isopycnals. Fine-scale sampling revealed distinct habitat partitioning of various planktonic taxa, resulting from a balance of physical and biological drivers in relation to the front.

© 2014 Elsevier B.V. All rights reserved.

## 1. Introduction

Planktonic organisms experience environmental gradients that likely influence the processes of aggregation, dispersal, and differential survival, resulting in plankton patchiness (Steele, 1978). Sharp gradients in temperature and salinity typically occur in the vertical direction; the subject of numerous recent studies using high frequency sampling (Deksheniaks et al., 2001; Greer et al., 2013; McManus et al., 2005). Strong horizontal gradients in water column properties can also occur, but are typically confined to areas of the ocean where two different bodies of water meet, known as fronts. Though not exclusively so, fronts are often associated with a variety of ocean topographies such as seamounts, canyons, and shelf-breaks (see Genin, 2004 for review). Despite their prevalence, the role of fronts in structuring plankton communities at fine scales (1 m to 10 m) relevant to predator–prey interactions is poorly understood.

Shelf-slope fronts are common along the western shelves of the world's oceans (Mann and Lazier, 2006) and serve as the boundary between relatively fresh shelf water and salty slope water (Houghton,

1997). These fronts are favorable habitat for a variety of organisms, having been shown to be associated with increased productivity in phytoplankton, zooplankton, and fish (Fournier et al., 1977; Mann and Lazier, 2006). To explain shelf-slope front productivity, Chapman and Lentz (1994) created a numerical model that described the circulation and predicted that bottom boundary convergence maintained the stability of the front. The convergence leads to upward flow of water along seaward sloping isopycnals, which increases nutrient input into near surface waters and consequently, phytoplankton productivity (Gawarkiewicz and Chapman, 1992). Experimental dye injections into the bottom boundary layer confirmed that convergence and along-isopycnal upwelling occurs in the field (Houghton, 1997). Biophysical models predicted that zooplankton production at the shelf-slope front could suppress phytoplankton biomass, but overall primary production in the front was high due to the consistent upwelling (Zhang et al., 2013).

Upwelling flows near the shelf-break enhance biological productivity for a variety of taxa in addition to the phytoplankton. For primary consumers, upwelling at the shelf-break leads to phytoplankton production and a favorable feeding environment for grazers including salps, copepods, and appendicularians. The increased secondary production at fronts can allow larval fishes to access high concentrations of prey (Bakun, 2006; Miller, 2002). On the other hand, fronts also can concentrate

\* Corresponding author at: University of Georgia, Boyd Graduate Studies 708A, 200 D.W. Brooks Drive, Athens, GA 30602, United States.  
E-mail address: [atgreer@uga.edu](mailto:atgreer@uga.edu) (A.T. Greer).

potential predators of larval fishes, such as hydromedusae and ctenophores (McClatchie et al., 2012). Gelatinous zooplankton are osmoconformers that actively reduce their swimming speed and aggregate near salinity gradients, which are a characteristic of shelf-edge ocean systems (Graham et al., 2001; Jacobsen and Norrbin, 2009). Salps, unlike hydromedusae and ctenophores, are bacteria and phytoplankton grazers that occupy a similar trophic niche as prey of larval fishes (copepods and appendicularians) but have reproductive rates similar to bacteria, much faster than copepods, appendicularians, and fish (Deibel, 1982; Deibel and Lowen, 2012; Heron, 1972; Tsuda and Nemoto, 1992). Therefore, salps could have an indirect negative impact on larval fishes by quickly consuming phytoplankton in a zone that is potentially favorable to secondary production of larval fish food sources (copepods and appendicularians). Salps can also negatively impact copepods directly by consuming them and their early life stages (Hopkins et al., 1993).

Most studies of planktonic organisms around frontal features have examined mesoscale patterns, detecting changes in average zooplankton and larval fish concentrations on either side of a front (Govoni and Grimes, 1992; Kingsford and Suthers, 1994; Nielsen and Munk, 1998; Sabatés et al., 2010). While these studies are useful in describing the shifts in plankton communities at fronts, they do not reveal much about small scale structure relevant to predator–prey interactions, so more recent frontal research has emphasized finer scale observations (Landry et al., 2012; Luo et al., 2014; McClatchie et al., 2012; Munk, 2014). The interactions of predators and prey at these fronts are largely unknown mainly because spatio-temporal patterns have not been resolved on the relevant scales of these associations. Small scale feeding environments have been shown to be extremely important to larval fish survival (Davis et al., 1991; Vlymen, 1977), yet remain a critical gap in our knowledge of the biological impact of many oceanographic features. In addition, the diversity of grazers and the biases of net based sampling systems to crustacean zooplankton (Alldredge and Madin, 1982; Remsen et al., 2004) obscure the fine-scale distribution of grazers and potential predators, thereby limiting the detectability of zones of the water column potentially favorable to larval fish feeding and survival.

New imaging technology is addressing some of the fundamental issues with sampling larval fishes and the surrounding biological community by quantitatively describing plankton in relation to fine-scale environmental variables that characterize shelf-slope boundaries. A distinct advantage of optical systems is the ability to automatically count and size marine particles using image analysis software. Particle size and abundance provide a suite of information relating to trophic interaction, reproduction, and carbon export to deeper waters (Sheldon et al., 1972; Stemmann and Boss, 2012; Woodward et al., 2005). In addition, the metric equivalent spherical diameter (ESD) commonly used in particle size estimation may not be applicable in coastal waters where particles (marine snow) vary in shape, composition, and optical properties (Kranck and Milligan, 1991). The *In Situ* Ichthyoplankton Imaging System (ISIS) combined with image analysis software allows for the automated counting, sizing, and simple feature extraction of particles, while providing the resolution adequate for the identification of many specimens to the family or genus level. The central goal of this study was to quantitatively describe the fine-scale abundances of larval fishes, gelatinous zooplankton, and particles of different size classes and composition, and use this high resolution data to better understand biological interactions at sharp physical gradients associated with the shelf edge.

## 2. Methods

### 2.1. Imaging system

The *In Situ* Ichthyoplankton Imaging System (ISIS) was used to quantify a variety of planktonic organisms in the size range of 680  $\mu\text{m}$  to 13 cm. ISIS utilizes a Piranha II line scan camera (Dalsa) to shoot a

continuous image with a scan rate of 36,000 lines  $\text{s}^{-1}$ . The images are produced by projecting collimated light across an imaged water parcel, and plankton blocking the light source are imaged as shadows, allowing for a range of transparent (gelatinous) and opaque (crustaceans) organisms to be imaged with no discernible bias in detectability (Cowen and Guigand, 2008; Cowen et al., 2013). Although ISIS shoots a continuous image, software (Boulder Imaging, Inc.) breaks up the image into 13 cm  $\times$  13 cm frames with a 40 cm depth of field. At typical tow speeds of 2.5  $\text{m s}^{-1}$ , it takes approximately 7.7 s to sample 1  $\text{m}^3$  of water. ISIS was also equipped with motor actuated fins for depth control, a Doppler velocity log (600 micro, Navquest) and environmental sensors including a conductivity, temperature, and depth sensor (CTD) (SBE 49, Seabird electronics) and fluorometer (ECO FL (RT), Wetlabs chlorophyll-*a* fluorescence). The CTD and fluorometer sampled  $\sim$ 30 cm and  $\sim$ 1 m above the imaged water parcel, respectively.

### 2.2. Sampling scheme

Two ISIS transects were performed in the same location on separate sampling days in August 2010, beginning on the shelf in waters approximately 75 m deep during different stages of the tidal cycle. The transect on August 27 was performed between 0710 and 1348, spanning 60.1 km, while the transect on August 29 was slightly shorter, lasting from 1656 to 2248 for a total distance of 52.7 km. The August 27 transect was performed during the flood tide, and the August 29 transect was during ebb tide, though tides were expected to have little effect near the shelf edge. Transects occurred in the shelf-break zone east of Georges Bank, off the coast of Massachusetts, USA, where there are consistent horizontal gradients in salinity and temperature (Fig. 1).

### 2.3. Bongo net samples

After each ISIS transect, 3–4 net tows using a 61 cm bongo sampler with 335  $\mu\text{m}$  mesh size were performed along the transect path at approximately evenly spaced stations. A flowmeter was attached in the center of the bongo mouth opening to quantify the volume of water filtered by the net. A CTD (SeaCAT SBE 19) was also attached to the tow wire above the bongo net to measure environmental variables and real time depth of the sampler during deployment. The bongo tows were conducted following the method of Jossi and Marak (1983). For each tow, the wire was paid out at a rate of 50  $\text{m min}^{-1}$  to a depth of  $\sim$ 5 m above the bottom. The wire was then retrieved to the surface obliquely at 20  $\text{m min}^{-1}$  while the ship was moving at 0.75–1  $\text{m s}^{-1}$ . At the end of each tow, the bongo net was brought on-board and samples were rinsed onto a 333  $\mu\text{m}$  sieve, and then preserved in 95% ethanol. After 24 h, sample ethanol was replaced with fresh 95% ethanol to enhance preservation. Samples were then shipped to the Plankton Sorting and Identification Center in Szczecin, Poland for sorting, identification, and measurement.

### 2.4. Image processing

ISIS images were viewed and analyzed in ImageJ (v1.46r, Rasband, 1997–2012). Prior to analysis, images underwent a standard ‘flat-fielding’ procedure to remove background variation and vertical lines from the line scan imaging. All images were viewed manually, and larval fishes were identified to the family level, with species level identification made possible by examining the taxa captured in the bongo nets. Standard length was measured in pixels and converted to mm using the known pixel resolution and field of view. A potential source of small measurement error was the orientation of the larval fish relative to the camera ( $\pm$  200–300  $\mu\text{m}$ ), but this was not quantified. For each ISIS downcast, gelatinous organisms, including salps, hydromedusae (*Clytia hemisphaerica* and *Persa incolorata*), ctenophores (lobate ctenophores and *Beroe* spp.), and siphonophores, were identified to the lowest taxonomic level possible (typically at least to family level).

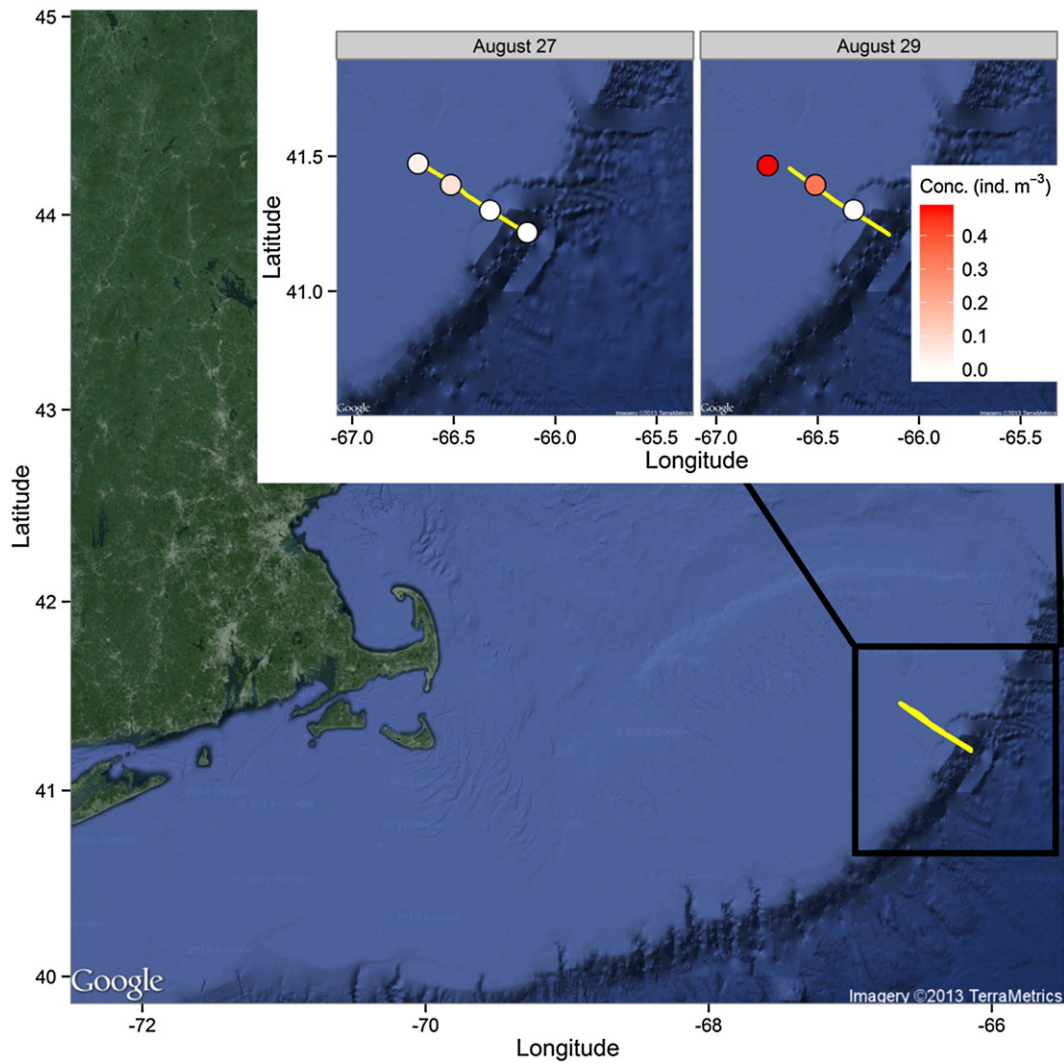


**Fig. 1.** Map showing the location of the two ISIS transects sampled on the eastern side of Georges Bank, Massachusetts, USA. Inset map displays the location of the bongo samples with color corresponding to the concentration of fish larvae.

For the colonial salps, counts of organisms per colony were made, and it was noted if only part of the colony was in the image frame.

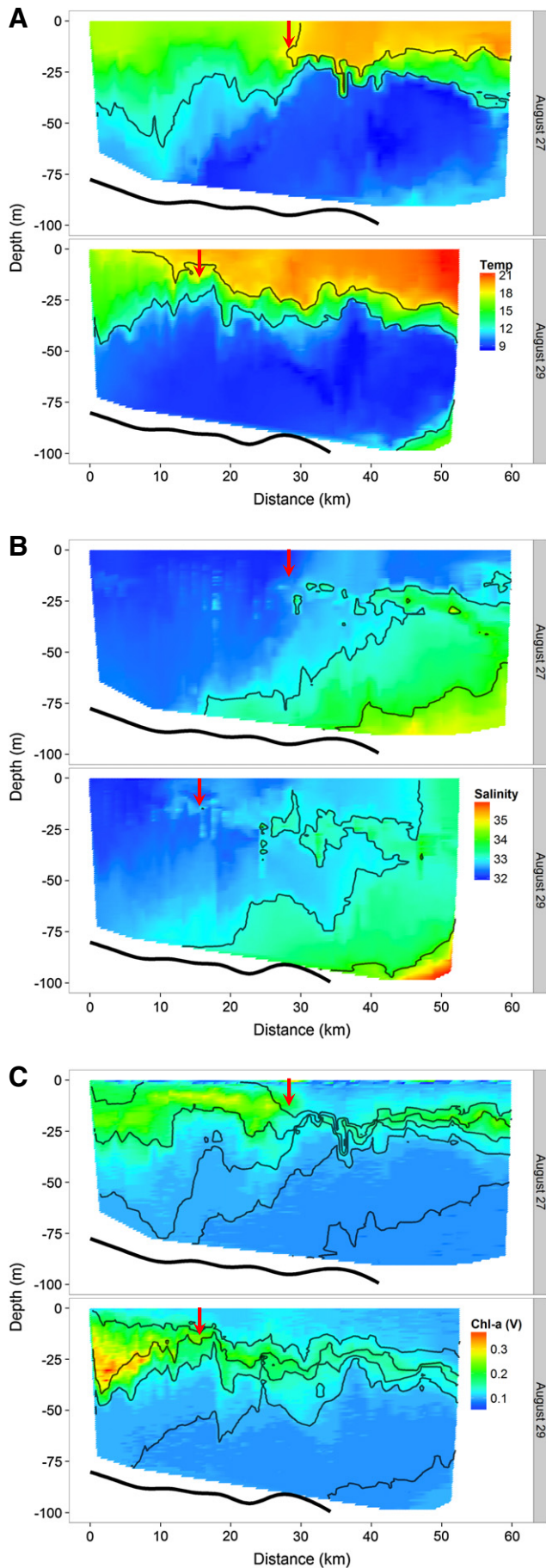
Counts of particles (predominantly diatoms and marine snow) were made using a custom ImageJ macro, which automated a series of tasks. The program first thresholded the 8-bit grayscale image by converting pixels with a gray level  $\leq 170$  to black and  $> 170$  to white. This global threshold was determined by trial and error to remove most of the faint gray lines associated with the line scan camera (produced by tiny dust particles on the camera lens). Then, utilizing ImageJ's 'Particle Analyzer,' particles were enumerated in three different size classes based on pixel area of the particle corresponding to different plankton groups. Size was measured using the cross-sectional area (in pixels) measured by the number of white and black pixels within a black pixel contiguous border. The size classes were defined by running the particle counter on human identified images, and making size classes based on differences in taxon-specific size frequency histograms. The 100–400 pixel size class (0.25–1.00 mm<sup>2</sup> cross-sectional area) corresponded mostly to diatom chains, small copepods, and small marine snow aggregates. The 401–1200 pixel size class (1.003–3.000 mm<sup>2</sup> cross-sectional area) consisted of larger copepods, appendicularians, and large marine snow aggregates. Particles in the 1201–5000 pixel size range (3.003–12.500 mm<sup>2</sup> cross-sectional area) targeted chaetognaths and shrimps (and the occasional fish larva). To further differentiate between particles within size class, a solidity metric

was used to distinguish organisms with an exoskeleton (high solidity), appendicularians (intermediate solidity), and loosely aggregated diatom flocs (low solidity).

$$\text{Solidity} = D/C \quad (1)$$

where D is the area of black pixels within the object (after thresholding) and C is the total cross-sectional area of the entire object including the white and black pixels inside of a black pixel perimeter. Crustaceans, with their opaque exoskeletons, have solidity near 1, while diatom aggregates with uneven gray level in the images will have lower solidity (~0.2).

Image histogram statistics for each frame were used to remove images that likely had erroneous counts. Images with mean pixel gray levels of  $< 221$  and pixel standard deviation  $> 42$  contained artificially inflated particle counts and were discarded. These histogram statistic limits were determined using trial and error on a variety of different image types throughout the transects. Even with this filtration procedure, many of the images seaward of the front had artifacts from passing through strong density discontinuities. The use of solidity to distinguish these artifacts from actual particles was tested by manually examining portions of the water column with different particle solidities.



## 2.5. Data analysis and statistics

ISiS sensor data (temperature, salinity, relative chlorophyll-*a* fluorescence) underwent processing for quality control. 134 chlorophyll-*a* readings (0.18%) and two temperature readings (0.0028%) were removed because measurements were erroneous. Directional variograms (vertical and horizontal) were used to interpolate the sensor data and particle counts across the entire transect. Directional variograms and interpolation was performed in R (R Core Team, 2013, v2.15.2) using the packages “sp” (Bivand et al., 2008; Pebesma and Bivand, 2005), “gstat” (Pebesma, 2004), and “Akima” (Akima et al., 2013). Kruskal–Wallis tests were used to assess differences in the mean depth among larval fish taxa.

A logistic Generalized Linear Model (GLM) with logit link function was used to examine the power of environmental variables to explain the probability of salp presence/absence. Logistic GLMs require a response variable that is binary or a proportion between 0 and 1 and can elucidate variables associated with changes in this response. The response variable was salp presence/absence with relative chlorophyll-*a* fluorescence and distance to the front as predictor variables. Temperature and salinity were not used in the model because of strong correlation between temperature and relative chlorophyll-*a* fluorescence (0.693 Spearman rank correlation) and little change in salinity where most salps were found. The main goal of the logistic model was to see if there was a relationship between salps and their prey (measured as relative chlorophyll-*a* fluorescence), and including many correlated variables would obscure this relationship. The front was located by visually inspecting the point where isopycnals flattened and reached their closest vertical distance. During the summertime, thermal stratification prevents the isopycnals from reaching the surface (Houghton et al., 2009). Salps from both sampling days were pooled and placed into 1 m<sup>3</sup> bins, and environmental variables were averaged for each bin. The model was fit in R (v2.15.2, R Core Team) and assessed using Akaike’s information criterion (AIC). Z tests were used to assess the significance of model coefficients, and residual deviance changes indicated the goodness of fit.

To assess the relationships of the different zooplankton taxa to all of the variables measured simultaneously, a correspondence analysis (CA) was performed using the R package “vegan” (Oksanen et al., 2013). Both sampling days were pooled because of strong similarities in zooplankton distributions. All zooplankton occurrences were binned into 1 m<sup>3</sup> bins (19.25 m horizontal distance), with environmental parameters (temperature, salinity, oxygen, relative chlorophyll-*a* fluorescence, and depth) being averaged across each m<sup>3</sup> bin. Only environments with at least 1 zooplankton present were used in the CA because large portions of the transects contained no zooplankton targeted by manual analysis.

## 3. Results

### 3.1. Mesoscale (bongo) sampling for fish larvae

The abundance of larval fishes captured in the bongo nets showed dramatic differences between the two sampling days. On August 27, a total of 23 larvae were captured (0.03 ind. m<sup>-3</sup>), while on August 29, 123 larvae were captured (0.17 ind. m<sup>-3</sup>), including 61 individuals on the most inshore bongo sample (0.48 ind. m<sup>-3</sup>, Fig. 1). Bongo samples were dominated by *Urophycis* spp. and *Merluccius bilinearis* (47.9% and

**Fig. 2.** Environmental data collected with ISiS sensors along two transects from northwest to southeast across a front. The smooth black line at the bottom of each panel shows the location of the bottom. A) Temperature with the 12 and 18 °C isotherms in black. B) Salinity with the 33 and 34 isohalines in black. C) Chlorophyll-*a* fluorescence (volts) with the sigma-*t* contours shown in black (23.7, 24.0, 24.7, 25.3, 26.0 isopycnals). Location of the front is indicated by red arrows.

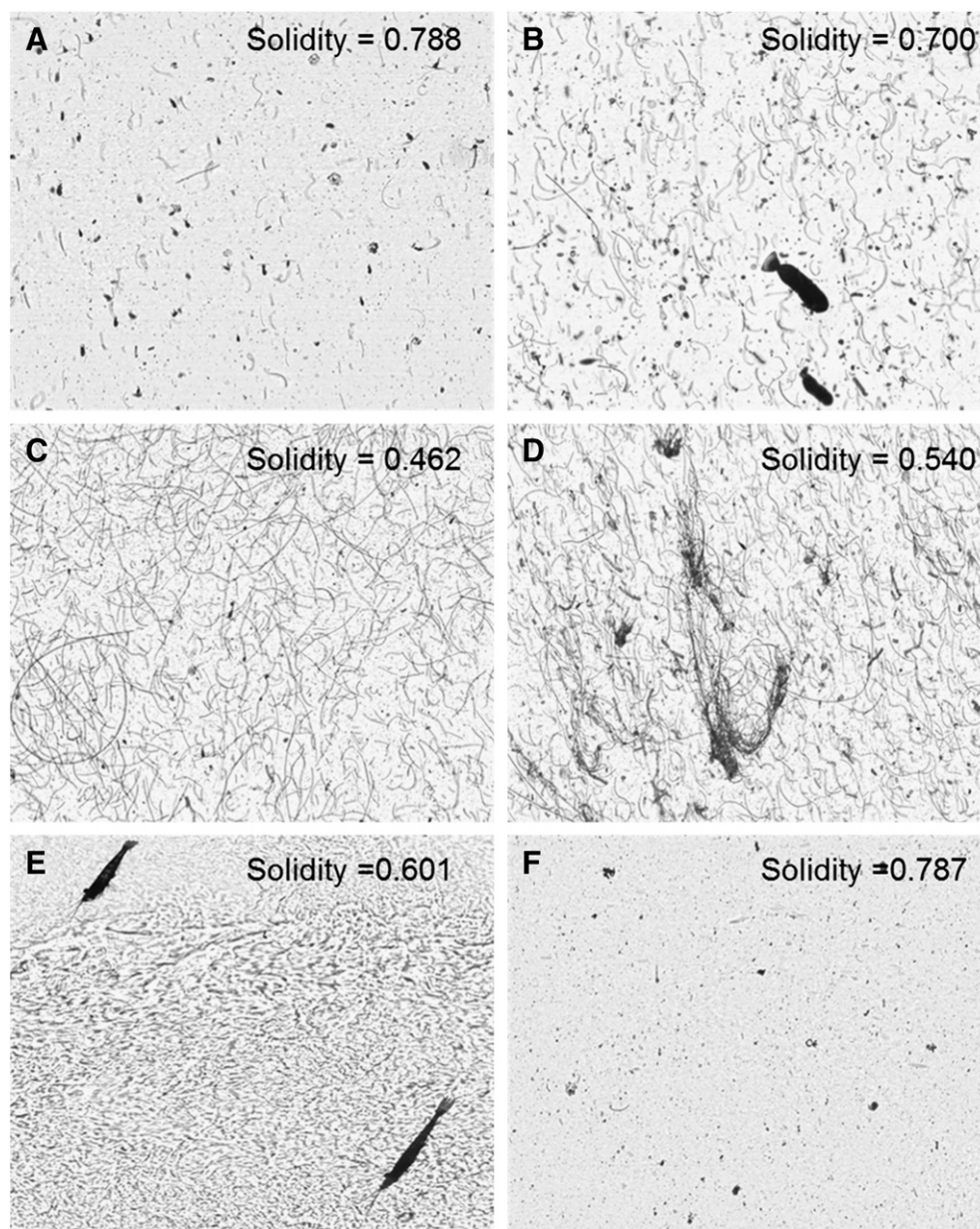


**Fig. 3.** Example images from different parts of the water column with average particle solidity per frame: A) near-surface copepod aggregations; B) near-surface mixture of zooplankton and diatom chains with two *Urophycis* spp. larvae; C) high concentrations of diatom chains in zone of high chlorophyll-*a* fluorescence; D) diatom aggregate formation at base of chlorophyll maximum; E) turbulence whirls and two euphausiids associated with slope water density discontinuities and low overall zooplankton abundance; and F) particles of unknown origin in deep waters (100 m).

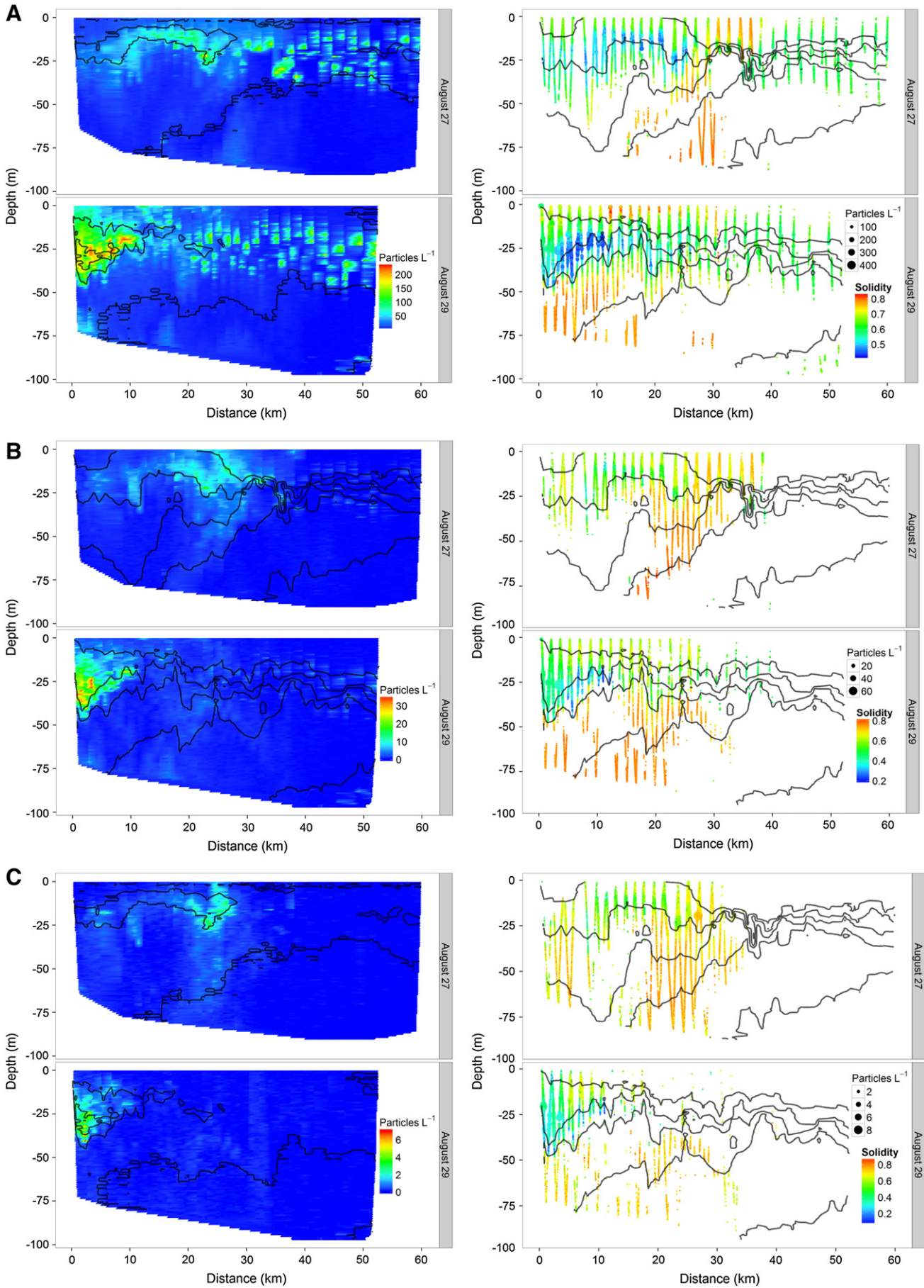
33.6%, respectively). Salps were also abundant in the bongo nets on the shelf side of the front but were not quantified.

### 3.2. Fine-scale physical setting

The sampling area was marked by strong shifts in temperature and the vertical positioning of isotherms (Fig. 2A). On August 27, the temperature on the shelf edge below the pycnocline was 9–10 °C (between 15 and 50 km into the transect). This cold water had moved shoreward on August 29, relative to its August 27 position. Waters on the shelf tended to be cooler at the surface and less thermally stratified compared to the slope waters. Moving offshore, isotherms shoaled near the pycnocline, forming highly stratified waters near the shelf edge and slope (~30 km on August 27, ~18 km on August 29).

Changes in salinity were the most apparent physical characteristic defining shelf and slope waters at the front. Salinity was relatively uniform throughout the water column during the first 10–15 km of the transects. Around 15–20 km into the transects, isohalines began to slope upwards and seaward, and salinity intrusions of slope water onto the shelf occurred along the pycnocline at ~25 m depth (Fig. 2B). Higher salinity levels were seen on August 29, potentially due to the movement of colder slope water onto the shelf. Most sampling took place inshore of and within the shelf-slope front, but we did not sample the surface of the shelf-slope front, which is typically defined by the 34.5 isohaline (Linder et al., 2006; Mountain, 2003) and sometimes does not reach the surface in the summertime (Houghton et al., 2009).

The combination of temperature and salinity created shifts in water density that were closely connected to the vertical and horizontal distribution of relative chlorophyll-*a* fluorescence (Fig. 2C). Similar to



isotherms, isopycnals shoaled as the 12 °C isotherm reached its shallowest depth of 15–20 m (distance of 30 km on August 27 and 20 km on August 29). Most of the relatively high chlorophyll-*a* fluorescence above 0.2 V was contained between the 23.3 and the 24.7 isopycnals, with generally lower and a much more limited vertical extent of chlorophyll-*a* fluorescence in the stratified slope waters found ~30 km into the transects. Deep isopycnals generally sloped upward and seaward in a similar direction to isohalines, but, unlike isohalines, flattened out when reaching ~25 m, a depth where the vertical temperature and density gradients were sharpest. The flattening of isopycnals occurred at a transect distance ~30 km on August 27 and ~20 km on August 29.

### 3.3. Particle distributions and solidity

Particles in the 100–400 (0.25–1.00 mm<sup>2</sup> cross-sectional area) pixel size range generally consisted of small diatom aggregates and small copepods, and particle solidity was used to distinguish between these groups (Fig. 3). Particles were most abundant before convergence of isopycnals (i.e. the shoreward side of the front) and strongly overlapped with the distribution of relative chlorophyll-*a* fluorescence (Fig. 4A). The solidity metric revealed changes in the dominant constituents of these particles. Particles with low solidity were found within areas of high relative chlorophyll-*a* fluorescence and were visually confirmed to be dominated by diatoms. A subsurface layer of high solidity occurred a few meters above the convergence of isopycnals on both sampling days (most pronounced on August 29, 15–25 km), and was dominated by copepods with very few diatoms imaged in this area. Appendicularians were also common in this subsurface layer, especially on August 27, but many occupied the larger particle size class. Particles in deeper waters (>30 m) with high solidity were mostly dense, opaque marine snow, with very few copepods (22–30 km on August 27, 0–20 km on August 29). The 100–400 pixel size class was contaminated with image artifacts near strong density gradients (caused whirls in the images). These artifacts were counted as particles in zones of strong density stratification. The artifacts are indicated by solidity near 0.6 and proximity to several isopycnals, occurring primarily in offshore stratified waters <35 km into the transects (sporadic high counts, Fig. 4A).

Particles from 401 to 1200 pixels (1.003–3.000 mm<sup>2</sup> cross-sectional area) were mostly larger diatom aggregates, larger copepods, and appendicularians (Fig. 4B). The highest abundance of these particles also occurred near the chlorophyll-*a* maximum, with twice the maximum abundance occurring on August 29 compared to August 27. August 27 showed more size separation, with particles in the 401–1200 pixel size range being more abundant close to the front and near surface, corresponding with zooplankton aggregations. Particle solidity measurements provided further evidence of crustaceans and appendicularians aggregating near surface above the isopycnals convergence. The chlorophyll-*a* maximum was dominated by loose diatom aggregates (low solidity), and deep waters (>30 m) on the shoreward side of the front were once again populated by dense marine snow aggregates (high solidity, distances of <30 km).

Particles in the size range of larger zooplankton (chaetognaths and shrimps) between 1201 and 5000 pixels (3.003–12.500 mm<sup>2</sup> cross-sectional area) were also dominated by aggregates, but showed different patterns in relation to the zone of high relative chlorophyll-*a* fluorescence between the sampling days (Fig. 4C). On August 27, most of these large particles were aggregated near the front (20–30 km), but on August 29, the particles were most abundant in the same area as the other particle size classes and zone of high chlorophyll-*a* fluorescence (0–15 km).

There was also a trend towards decreased solidity on August 29 compared to August 27. Similar to the other particle size classes, the solidity was lowest in areas where chlorophyll-*a* fluorescence was highest, indicative of large diatom aggregates in this zone.

### 3.4. Fine-scale larval fish abundance and distribution

In total, 223 larval fishes were found in ISIS images on the two sampling days, dominated by the families Merlucciidae (48.4%) and Phycidae (23.3%) (see Fig. 5 for example images) and confined to the shelf side of the front (Fig. 6). A portion of the larval fishes were not identifiable (12.1%) due to orientation and/or lack of detectable features, while 9.9% were preflexion larvae. Families under the order Pleuronectiformes were pooled due to low abundances. Merlucciidae and Pleuronectiformes larvae occupied significantly deeper waters than other taxa (Kruskal–Wallis test,  $P < .0001$ ). Phycidae larvae were shallower (Kruskal–Wallis test,  $P < .0001$ ) (Fig. 7), with preflexion larvae found in waters slightly deeper than Phycidae. Unlike the bongo sampling, no difference in larval fish abundance was found between the two sampling dates; however, the first ISIS profile on August 29 contained a concentration of 0.74 ind. m<sup>-3</sup>, corresponding to the same area of high abundances detected by the bongo net (0.48 ind. m<sup>-3</sup>).

Temperature/salinity diagrams in the context of larval fish presence/absence showed larval fishes occupying a fairly narrow range of salinity (almost absent when salinity was >33.0) but a larger range of water densities (Fig. 8). The 23.3 isopycnal was the only one along which larvae were found across a range of salinities on both sampling days. Larval fishes were found in zones where relative chlorophyll-*a* fluorescence and particle abundance were high (on the shoreward side of the front).

### 3.5. Salp abundance and distribution

A total of 49,161 salps, consisting of *Thalia democratica*, were found in the images, with 97.5% of those individuals being in colonial form. The highest abundances of salps occurred in shelf waters with intermediate levels of relative chlorophyll-*a* fluorescence, usually several meters shallower than the chlorophyll-*a* maximum on each profile (Fig. 9). Salps reached concentrations of over 5000 ind. m<sup>-3</sup> on several occasions, but were most concentrated on August 29, which had higher peak chlorophyll-*a* fluorescence. A few individuals were found in very deep waters (>70 m) and were likely dead and decaying since phytoplankton abundance in this area was low and dominated by dense marine snow aggregates.

A logistic regression revealed a significant impact of relative chlorophyll-*a* fluorescence and distance to the front on the probability of salp presence (Table 1). The model showed the highest probability of presence occurred at intermediate levels of fluorescence, similar to those found several meters above the chlorophyll-*a* maximum (Fig. 10). Salps were accurately predicted to be absent within and seaward of the front, regardless of the chlorophyll-*a* fluorescence in these zones. Goodness of fit was measured as a 10.6% reduction in the residual deviance.

### 3.6. Gelatinous zooplankton distributions

The most abundant gelatinous zooplankton other than salps were the hydromedusae *C. hemisphaerica* and *P. incolorata* (images in Fig. 5). Maximum concentration detected for these two species was 167 ind. m<sup>-3</sup> and 90 ind. m<sup>-3</sup>, respectively. Distributions of the

**Fig. 4.** Particle counts in three different size classes and solidity of particles counted. The left panels show particle concentration with chlorophyll-*a* fluorescence drawn in black. Panels on the right show particle solidity above a certain minimum concentration for each size class with density contours drawn in black (23.7, 24.0, 24.7, 25.3, 26.0 isopycnals). The size of the point corresponds to particle concentration in that area with low concentrations removed for clarity purposes. A) 100–400 pixel size class (concentrations of >4 particles L<sup>-1</sup>), B) 401–1200 pixel size class (concentrations of >0.5 particles L<sup>-1</sup>), C) 1201–5000 pixel size class (concentrations of >0.1 particles L<sup>-1</sup>).



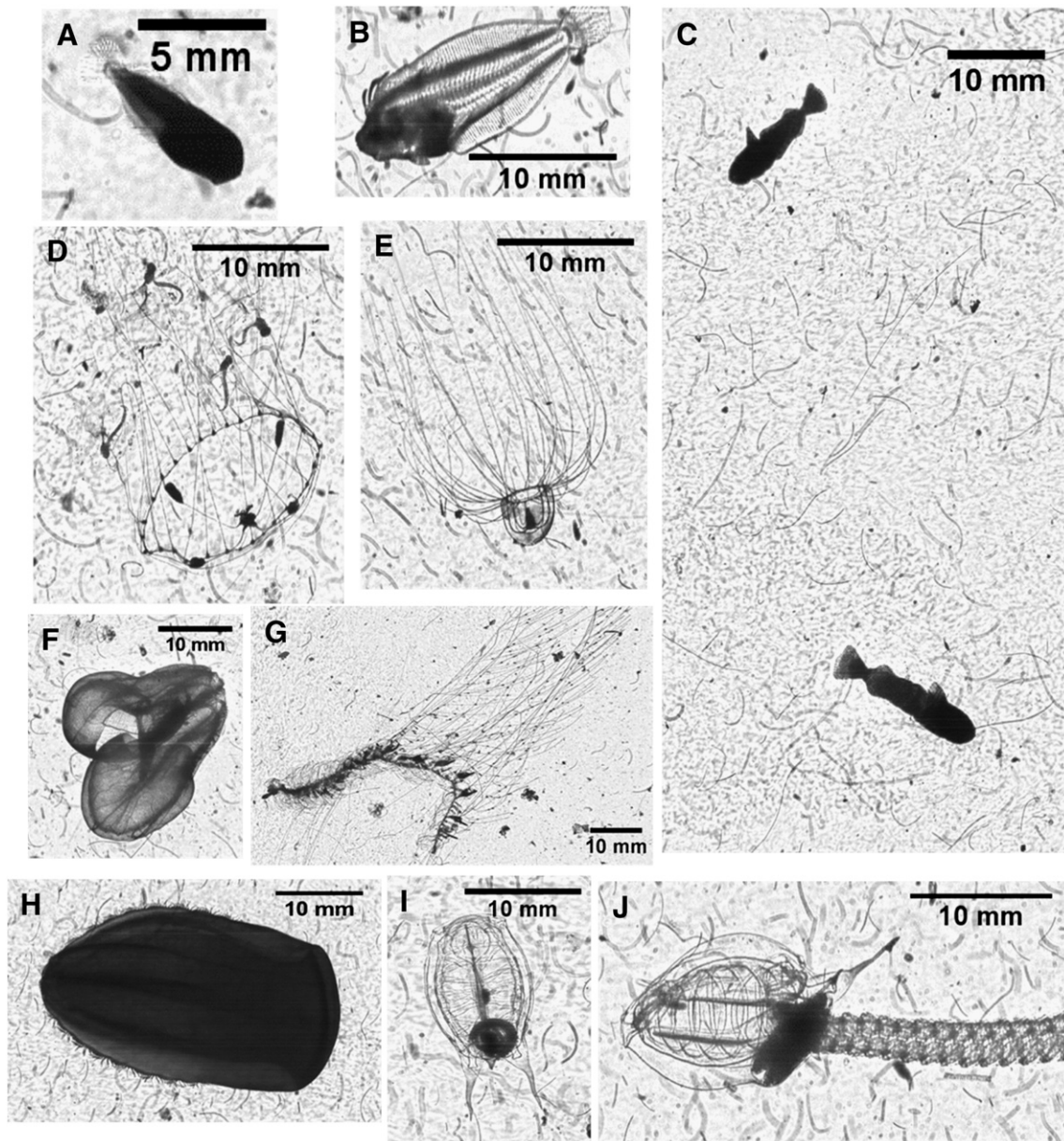


**Fig. 5.** Example ISIS images. A) Phycidae larva. B) Pleuronectiformes larva. C) Two Merluccidae larvae. D) *Clytia* spp. hydromedusa. E) *Persa* spp. hydromedusa. F) Lobate ctenophore (*Bolinopsis* spp.). G) Siphonophore. H) *Beroe* spp. I) Solitary salp *Thalia democratica*. J) Solitary-stage zooid of *Thalia democratica* producing a new chain of aggregate zooids.

hydromedusae tended to follow isopycnals, with highest abundances between the 23.8 and 23.3 isopycnals. Both species were not concentrated at the front and were virtually absent seaward of the front (Fig. 11A, B).

Ctenophores and siphonophores displayed remarkably different vertical distributions from the hydromedusae, with the two ctenophore groups occupying opposite extremes in depth. Similar to other zooplankton, ctenophores and siphonophores were most abundant on the shoreward side of the front. Lobate ctenophores, consisting mostly of *Bolinopsis* spp., were common in surface waters and showed signs of limited depth distribution based on the 23.3 isopycnal (Fig. 11C). The miscellaneous ctenophores, mostly consisting of *Beroe* spp., were more common in deeper waters, and spatial patterns did not follow isopycnals (Fig. 11D). Siphonophores were much less abundant overall, but aggregated at the surface near the front on August 29 (Fig. 11E).

The correspondence analysis showed many of the zooplankton taxa clustering in environments characterizing the shelf waters. This is not surprising considering that most taxa were found on the shelf side of

the front in relatively shallow water. Polychaetes separated from the other zooplankton, being found in deeper and more saline waters (Fig. 12A). The miscellaneous ctenophore group (mostly *Beroe* spp.) was found in the deepest waters and therefore was impossible to visualize well with the other zooplankton groups. Zooming in on the shelf-associated zooplankton groups, it is apparent that the two hydromedusae groups (H and H2, *C. hemisphaerica* and *P. incolorata*) were found in the shallow waters with the lowest salinity and highest temperatures. The other gelatinous groups separated in relation to salinity (groups arranged roughly parallel with respect to the salinity axis), which makes sense because the siphonophores were generally found closest to the front where salinity began to increase (Fig. 12B).

#### 4. Discussion

Distributions of larval fishes, chlorophyll-*a* fluorescence, diatom aggregates, copepods, appendicularians, and gelatinous zooplankton near a front showed strong vertical patterns often associated with

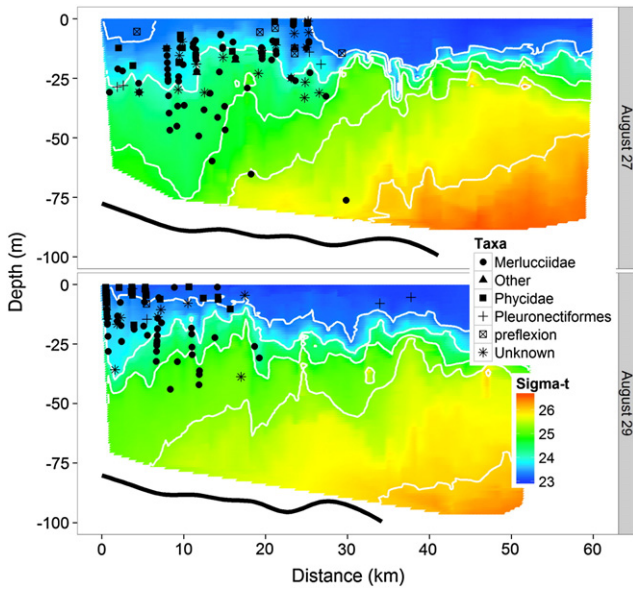


Fig. 6. Location of larval fish taxa in relation to water density (sigma-t) along transects sampled on two different days. Each point is one individual larva.

isopycnals. Fine-scale abundances in the horizontal direction showed elevated abundances in the shelf waters with almost complete absence of target organisms in the stratified slope waters. Particles of varying composition showed distinct associations with certain portions of the front. Copepods aggregated at the surface near the convergence of isopycnals, and a large number of particles were found underneath the front, potentially contributing to the export of organic material into deeper waters. Previous studies of shelf-slope fronts have not documented these detailed associations because of coarse sampling resolution (Albaina and Irigoien, 2004; Fernández et al., 1993; Munk et al., 2003) or inability to detect gelatinous organisms in these features that, based on high abundances, are likely important grazers (salps) and larval fish predators (hydromedusae and ctenophores). This and previous studies of fine-scale features demonstrate the importance of fine-scale environmental heterogeneities in determining the abundance and spatial extent of many zooplankton taxa. The following discussion will transition from a description of the physical environment at the front and move through the food web, starting with the distribution of

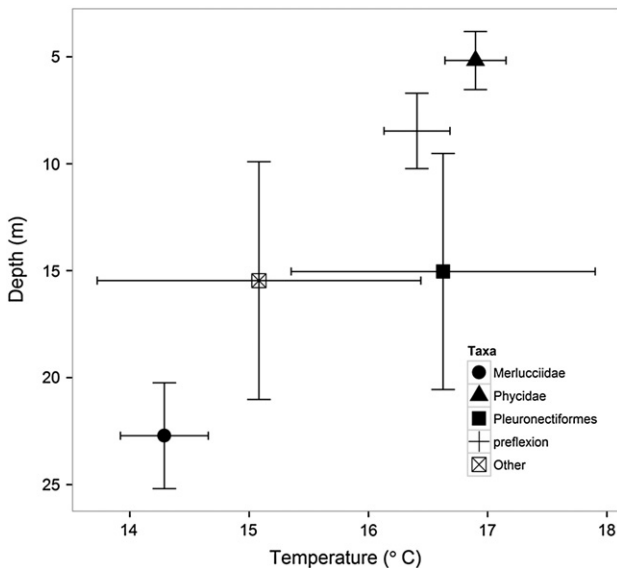


Fig. 7. Mean depth and temperature occupied by each larval fish taxon ( $\pm 1.96$  SE).

chlorophyll-*a* fluorescence, diatom particles, and grazers, to larval fishes and zooplankton predators.

#### 4.1. Physical environment at the front

Seaward sloping isopycnals merging near the pycnocline were consistent with previous studies at the shelf-slope fronts. Our study also documented a front defined by a weak surface temperature gradient and convergence of isopycnals. The mechanisms of formation of the temperature front are unclear, but could be related to an interaction between the shelf-slope front and offshore forcing (e.g., warm-core ring or Gulf Stream meander, Gawarkiewicz et al., 2012), interactions with the tidal-mixed front on Georges Bank (Loder et al., 1993), or upwelling of deep shelf water has been found to occur along these isopycnals (Marra et al., 1990). Average upwelling velocity is typically  $17.5 \text{ m d}^{-1}$ , depending on the steepness of the isopycnal slopes (Barth et al., 2004). The shoaling of isopycnals near 20–30 m depth during the summer has been suggested as a mechanism for favorable cross-front exchange (Houghton et al., 1988), but our finding of very few zooplankton on the oceanic side of the front despite the presence of high salinity intrusions suggests that cross-shelf exchange of zooplankton may only occur during the passage of warm core rings (Houghton et al., 1986). Strong diapycnal velocities at shelf-slope fronts indicate mixing across isopycnals (Barth et al., 2004; Houghton and Visbeck, 1998), which may have been depicted in our images as whirls within the image near density discontinuities. This diapycnal mixing also led to inflated particle counts in the highly stratified slope waters, particularly in the smallest size range (100–400 pixels). Flattening of isopycnals at the thermocline during the summer stratified months has been documented previously (Barth et al., 2004; Houghton et al., 1988), with strongest density changes containing intrusions of salty slope water onto the shelf (Gordon and Aikman, 1981). Because many characteristics documented by ISIS were consistent with previous studies of the shelf-slope front, it is likely that frontal circulation patterns, including bottom boundary convergence, upwelling along isopycnals, and a strong southward flowing frontal jet (Chapman and Lentz, 1994; Houghton and Visbeck, 1998; Mann and Lazier, 2006), were occurring during this study.

#### 4.2. Distribution of primary producers and particles

Diatoms and dinoflagellates are common summer phytoplankton prey on the shelf for a variety of grazers including salps, copepods, and appendicularians (Ashjian et al., 2001; Malone, 1977; Norrbin et al., 1996). Physical coagulation of diatoms appeared to dominate in areas of high chlorophyll-*a* fluorescence, but the fluorescence signal was spatially distinct from the aggregations of grazers, which were in shallower waters. These shallow zones were potentially populated by dinoflagellates, which were too small to be imaged by ISIS. Copepods have shown strong fine-scale spatial overlap with dinoflagellates near Georges Bank in previous studies (Gallager et al., 2004). Diatoms, which were correlated with chlorophyll-*a* fluorescence, may not be nutritionally sufficient for copepods (Pierson et al., 2005), and when present in high concentrations, can even have deleterious effects due to the production of toxic aldehydes (Leising et al., 2005; Miralto et al., 1999; Tosti et al., 2003). It is unknown whether the concentrations present in our study would be sufficient to produce toxic effects.

Where light levels are favorable for phytoplankton growth, converging and upward-sloping isopycnals should be associated with the input of nutrient-rich deep water (Marra et al., 1990). In the present study, however, chlorophyll-*a* fluorescence and peak particle concentrations did not occur in these areas, suggesting that the chlorophyll-*a* maximum is more related to the aggregation of sinking particles than the active growth and production of phytoplankton most favorable to zooplankton grazing. Elevated chlorophyll-*a* fluorescence inshore of the shelf-slope front has been documented occasionally (Marra et al., 1982, 1990), and our results suggest that the aggregation of sinking

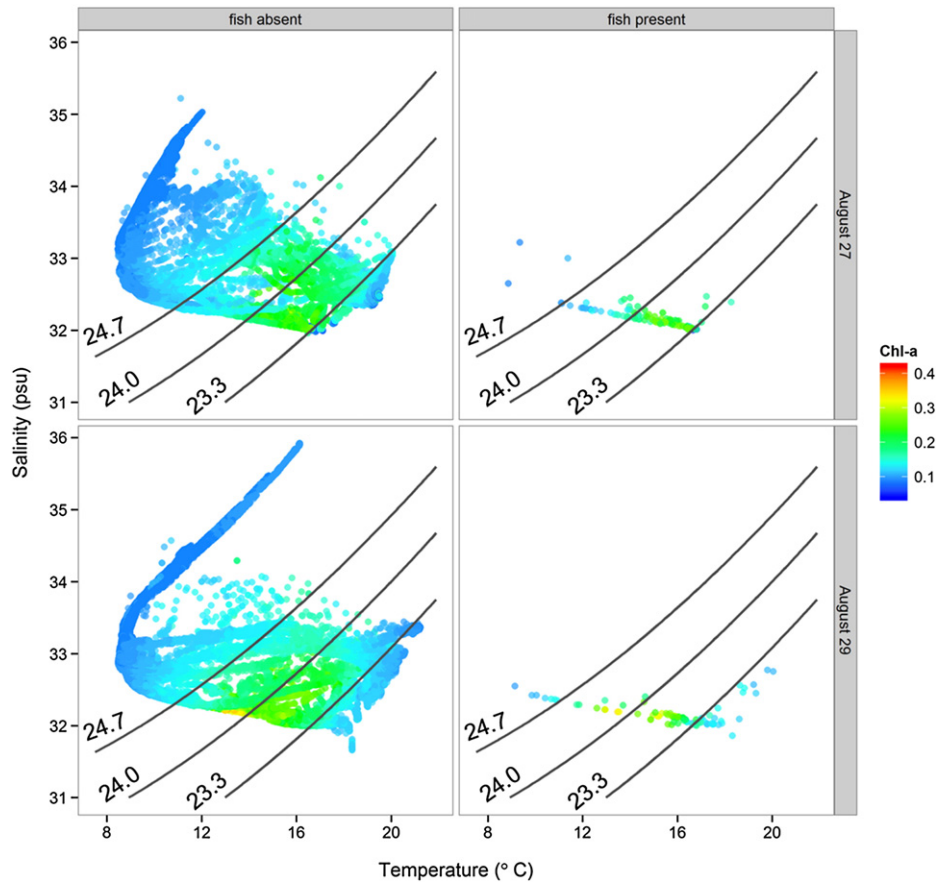


**Fig. 8.** Temperature/salinity diagrams of waters sampled with and without fish larvae on each of the two sampling days. The color of each point corresponds to the chlorophyll-*a* fluorescence (volts). Black lines are isopycnals.

diatoms at particular isopycnals could be responsible for this shift. This idea is supported by models of diatom coagulation, which predict that particles will become more aggregated with depth (Allredge and Gotschalk, 1989), causing particle size to increase and reach a maximum at the base of the photic zone (Jackson, 1990; Kiørboe et al., 1990). Further details on the surface circulation near the front and the

stickiness of diatoms in this region could reveal additional details on the mechanism behind this phenomenon.

4.3. Copepods, appendicularians, and salps

Phytoplankton grazers (salps, copepods, and appendicularians) were mostly found in waters several meters above high levels of chlorophyll-*a*. While salps were more abundant shoreward of the front at intermediate levels of chlorophyll-*a* fluorescence, copepods and appendicularians were dominant in surface waters above the front, with no particular relationship to chlorophyll-*a* or hydrographic variables (other than depth). Ashjian et al. (2001) quantified fine-scale distributions of copepods using the Video Plankton Recorder (Davis et al., 1992, 2005) across Georges Bank, finding high variability in abundances and little correlation with hydrographic variables, other than a slight negative correlation with chlorophyll-*a* fluorescence in the summer. Copepod behavioral experiments have shown that copepods are attracted to velocity gradients and show area-restricted searching (Woodson et al., 2005, 2007), potentially increasing their

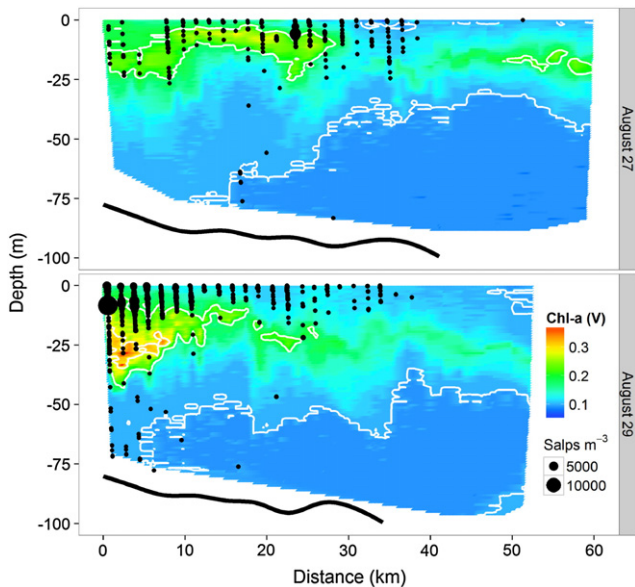


**Fig. 9.** Fine-scale distribution of salps (*Thalia democratica*) overlying chlorophyll-*a* fluorescence (volts). Chlorophyll-*a* contours are shown in white (0.1, 0.2, and 0.3 volt contours).

**Table 1**

Model coefficients on logistic regression of salp presence/absence in relation to chlorophyll-*a* fluorescence and distance to the front. Z values were used for Z tests to determine significance of the model coefficients. \*\*\* indicates a P value of < 0.001. Negative distances are shoreward of the front and positive distances are seaward.

Coefficient	Estimate	SE	Z value	Pr
Intercept	-8.012	2.812e-01	-28.50	***
Fluor	5.634e+01	3.688	15.28	***
Fluor <sup>2</sup>	-1.419e+02	1.096e+01	-12.94	***
Distance to front	-4.471e-05	2.517e-06	-17.76	***

Formula: Presence / Absence ~ Fluor + Fluor<sup>2</sup> + Distance to front.

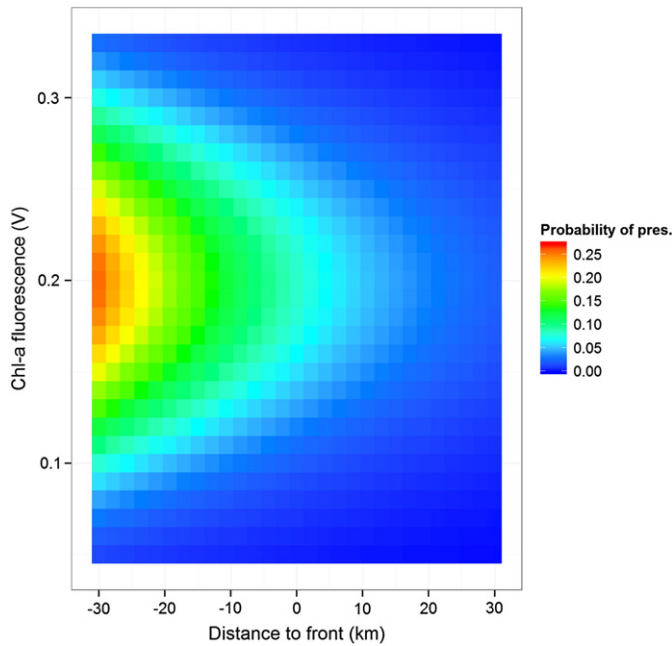


**Fig. 10.** Results of a logistic generalized linear model for salp presence/absence in relation to distance to front and chlorophyll-*a* fluorescence. Negative distances to the front are on the shelf side and positive distances are in slope waters.

encounter rates with prey items in these zones. The surface waters have also been shown to have the highest mean current speed in this region due to the strong surface frontal jet (Aikman et al., 1988; Mann and Lazier, 2006), and this zone has also been found to be populated with ciliates, another food item for copepods and potentially an understudied trophic link (Calbet and Saiz, 2005; Fernández et al., 1993). Gawarkiewicz et al. (1996) found highest along-isobath velocities at ~10 m in the frontal zone ( $0.51 \text{ m s}^{-1}$ , perpendicular to the ISIS transects), which would be just below the layer of copepods found on August 29. If the upwelling does indeed bring elevated nutrients and favorable conditions for dinoflagellate and/or ciliate growth combined with strong current velocity gradients, the surface waters above the front could be an ideal habitat for copepods. Higher resolution observations of smaller plankton ( $<400 \mu\text{m}$ ) would be needed to confirm whether the surface waters above the front are populated with smaller phytoplankton or microzooplankton that may be more important to copepod growth than diatoms (Calbet and Saiz, 2005; Pierson et al., 2005).

Shelf-slope fronts have been suggested as oceanographic features that would be particularly favorable for salp growth (Paffenhöfer and Lee, 1987), and our results provide support for this idea based on observed concentrations of salps being an order of magnitude higher than in previous studies in this region (Atkinson et al., 1978; Bathmann, 1988; Deibel and Paffenhöfer, 2009). Salps are capable of daily population doubling through asexual reproduction (Heron, 1972) and are able to filter large volumes of water to ingest prey across a range of sizes. Concentrations of other grazers are often negatively correlated with salps (Berner, 1967; Deibel, 1982; Fraser, 1962; Paffenhöfer et al., 1995), and our data revealed distinct spatial partitioning between salps and other grazing zooplankton.

The logistic GLM fit to salp presence/absence showed an association of these organisms to intermediate levels of chlorophyll-*a* on the shelf side of the front. When salps encounter particularly high concentrations of particles (and high chlorophyll-*a* fluorescence), their filters clog, stopping ingestion and greatly reducing their fitness (Alldredge and Madin, 1982; Harbison et al., 1986). Intermediate fluorescence levels (0.2 V in our study) may therefore represent a “goldilocks” amount of phytoplankton: sufficient for growth but not so much as to clog filters and decrease feeding efficiency. The well-mixed surface waters are

likely the site of growing diatoms which gradually coagulate and sink until reaching density discontinuities. The zones a few meters above the density discontinuities provide the opportunity of salps to feed before concentrations get too high near the pycnocline. Alternatively, this zone could be the productivity maximum with the phytoplankton of highest nutritional quality.

#### 4.4. Zooplanktivorous gelatinous organisms

Gelatinous zooplankton were abundant on the shelf side of the front, with taxon-dependent depth patterns often following isopycnal surfaces. The common hydromedusae sampled (*Clytia* spp. and *Persa* spp.) showed changes in their vertical distribution closely related to isopycnal depth. This is consistent with studies indicating that density discontinuities limit the movement of hydromedusae due to their inability to osmoregulate (Arai, 1976; Graham et al., 2001; Mills, 1984). Ctenophores also followed isopycnals, but the two groups were separated by depth. Lobate ctenophores aggregated in the surface waters with particularly high abundances near the surface intersecting with the 23.3 isopycnal. Other ctenophores (mostly *Beroe* spp.) were concentrated at depth and tended to be most abundant near the 25.0 isopycnal and in areas of lowest particle abundance. These ctenophores are known to have high clearance rates, and could potentially feed on marine snow aggregates exported from above the thermocline, as well as large copepods, euphausiids, and lobate ctenophores that venture to deeper waters (Haddock, 2007; Reeve et al., 1978; Toyokawa et al., 2003). Since some lobate ctenophores have been demonstrated to alter their swimming speed and vertical distribution in the presence of *Beroe* spp. predators (Titelman et al., 2012), the vertical separation between *Beroe* spp. and lobate ctenophores could indicate avoidance behavior or top down regulation.

The correspondence analysis biplot revealed separation between the different zooplankton groups. The two hydromedusae were found in essentially the same shallow, warm environment. However, the other taxa were found in slightly different environments, with salps, lobate ctenophores, and siphonophores being associated with increasing levels of salinity. Salinity could be a major driver of the fine-scale separation of these different taxa, while the hydromedusae could be in a situation of strong inter-species competition.

#### 4.5. Larval fish distributions and sampling technology

Fish larvae, many of which require copepods or nauplii for food, were found throughout the shallow shelf waters and were limited to relatively low salinities. Seaward of the converging isopycnals that marked the front, fish larvae were absent except for two individual Bothid larvae found near the surface. Due to the coarse resolution of most ichthyoplankton sampling, this strong association of larval distributions with particular physical features has not been previously documented. Phycidae larvae occupied the shallowest waters, and based on our particle counts and solidity measurements, likely encountered the highest concentration of zooplankton prey in this area. Merlucciidae larvae were found significantly deeper on both sampling days and are known to feed during the daytime on copepods up to 700  $\mu\text{m}$  in size (Cass-Calay, 2003; Sumida and Moser, 1980). The large eye lenses relative to the size of Merlucciidae larvae suggests that they are adapted to a wide range of light conditions (Morote et al., 2011), and therefore may rely on this stealthy behavior to feed successfully on lower concentrations of copepods at depth, whereas the distributions of Phycidae larvae suggests that they may require high concentrations of prey. Taxon-specific differences in habitat requirements have been suggested in many studies showing that larvae of different species thrive under different physical regimes (Buckley and Lough, 1987; Dower et al., 1998), but further study is required to determine if differences in food concentration affect species-specific condition.

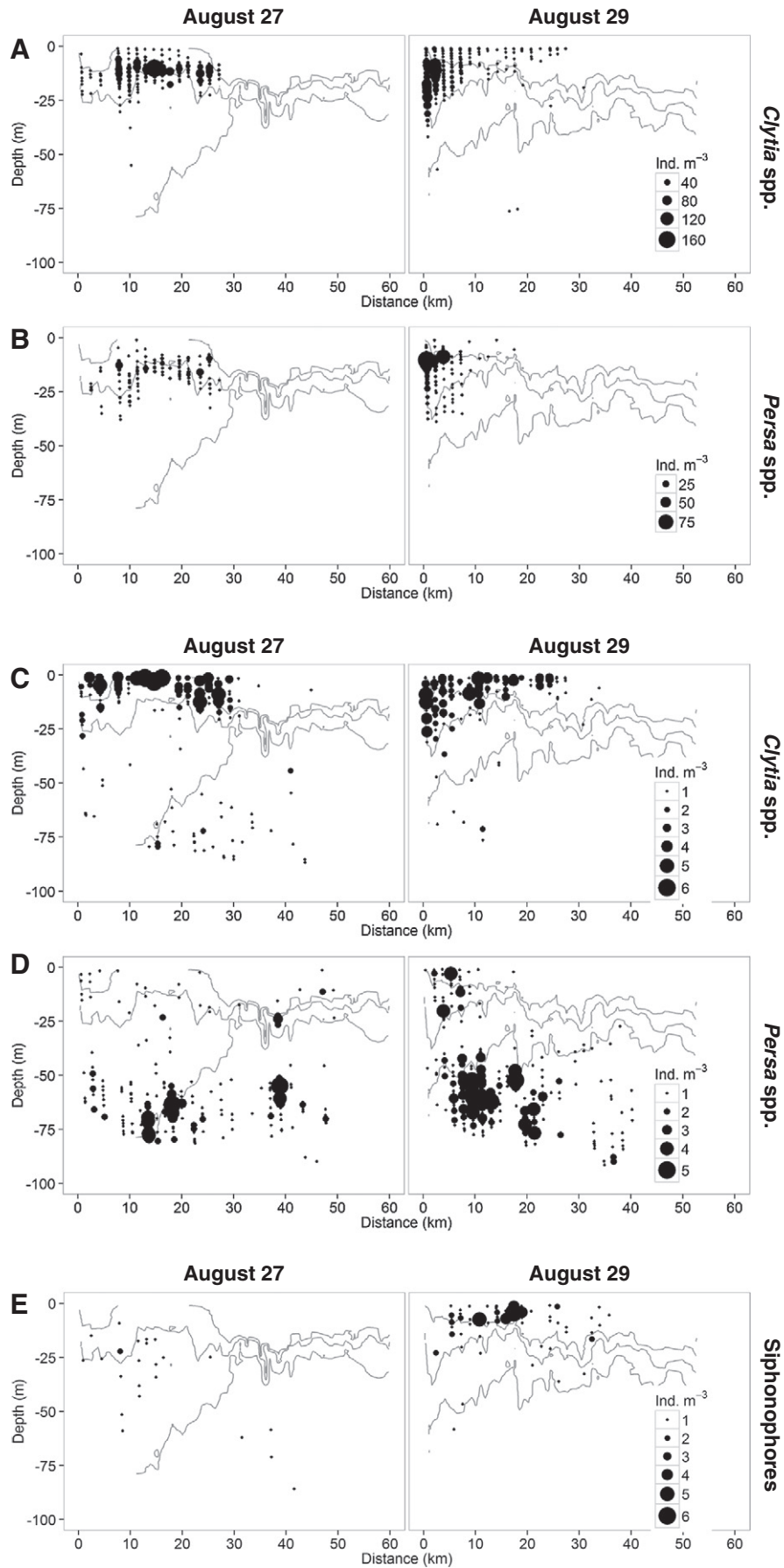


**Fig. 11.** Distribution of different gelatinous zooplankton in relation to the 23.3, 23.8, and 25.0 isopycnals. A) *Clytia* spp. B) *Persa* spp. C) Lobate ctenophores (*Bolinopsis* spp.). D) Miscellaneous ctenophores (mostly *Beroe* spp.). E) Siphonophores.

High larval abundances appeared to be associated with zones of the water column where isopycnals intersected with the surface, and larval distributions tended to follow the sloping isopycnals. Many studies have shown larval behavioral changes or aggregation in the vicinity of physical gradients, unrelated to the presence or absence of prey in these zones (Batty, 1994; Catalán et al., 2011; Clay et al., 2004; Lougee et al., 2002). Since prey patches have been shown to aggregate at density discontinuities (Bjørnsen and Nielsen, 1991), occupying these zones increases the chances of encountering high concentrations of prey items. Specifically, the upward sloping isopycnals and diapycnal velocities may be sites of velocity gradients or increased turbulence, potentially favorable for prey encounters (Kjørboe and MacKenzie, 1995; Rothschild and Osborn, 1988).

Larvae grow faster in warmer waters (Buckley et al., 1999; Houde, 1989; Pepin, 1991), but require adequate food resources to obtain this benefit. The slope waters had the warmest surface waters, but were virtually devoid of zooplankton prey for the fish larvae. The cold pool, which had very few fish larvae, also had few potential prey items and unfavorable conditions for larval growth. Thus, it is not surprising, given the horizontal shifts in both physical and biological conditions, that the upper half of the water column on the shelf side of the front was most populated with larval fishes.

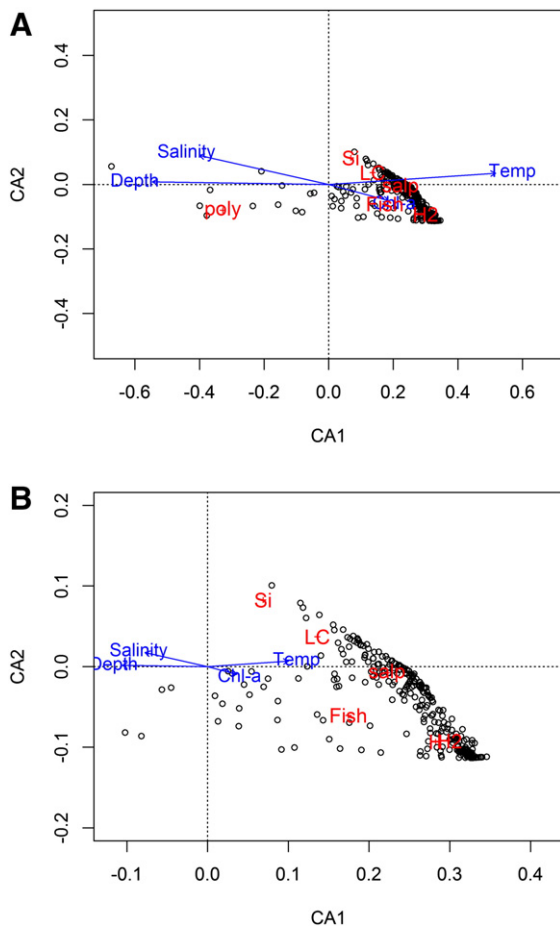


**Fig. 12.** A) Correspondence analysis (CA) for the different zooplankton taxa with a post hoc display of environmental variables (blue). Small black circles represent environments (each is  $1 \text{ m}^3$ ) where zooplankton were present. Taxa names are shown in red. Fish = fish larvae, salp = salps *Thalia* spp., LC = lobate ctenophores, H = hydromedusae *Clytia* spp., H2 = hydromedusae *Persa* spp., Si = siphonophores, poly = polychaetes. Miscellaneous ctenophore group (Cteno) not shown because they were found in much deeper waters. B) Zoomed in version of the same CA to show differences between taxa found in shelf waters.

In their relationship to potential predators, fish larvae showed spatial overlap with gelatinous zooplankton, providing little evidence of avoidance of these predators. It is apparent from these distributions that the primary driver of larval fish distributions is the distribution of prey, as all taxa which feed on zooplankton were most abundant on the shelf side of the front where particle concentrations were high. Given the extremely high concentrations of gelatinous zooplankton near aggregations of larval fishes, predator avoidance of these larvae on fine scales is likely a necessity. Controlled behavioral experiments would shed light onto how these larvae survive despite high concentrations of predators throughout their habitat.

The two sampling methods used for quantifying larval fishes showed distinct differences likely based on the timing of sampling and speed of instrument towing. Although ISIS has shown favorable comparisons to bongo nets during night sampling of fish larvae (Cowen et al., 2013), this study represents the first day/evening comparison of sampling techniques in the same area. While ISIS imaged roughly the same number of larvae during each of the two transects, bongo nets captured 5 times fewer larvae during the day sampling compared to the evening sampling. In the ISIS images, larvae tended to be large (8.1 mm average standard length), so it is likely that many of these larvae were able to avoid the bongo nets during the day, but were unable to avoid ISIS due to the fast tow speed ( $2.5 \text{ m s}^{-1}$  vs.  $0.75 \text{ m s}^{-1}$  for the bongo). During the night, as in the Cowen et al. (2013) study, the bongo nets and ISIS detected similar concentrations. ISIS may be a more effective ichthyoplankton sampler during daylight hours if the targeted larvae are older or have strong sensory and swimming abilities enabling net avoidance.

#### 4.6. Detailed events at the shelf-slope front and future directions

High-resolution particle counts revealed vertical and horizontal structure of plankton patchiness near shelf-slope fronts. The front itself clearly acted as a barrier to the movement of shelf water onto the slope, with strong stratification on the slope side of the front and very low abundances of plankton and particles. Patterns in sigma-t showed surface shoaling isopycnals at the front, likely related upwelling and increased productivity. At the front, there was an increased abundance of particles in deeper waters below the pycnocline, and also high abundances of zooplankton at the surface. The source of these particles is not known, but it could be a mixture of salp or copepod fecal pellets and dead or decaying diatom aggregates. These particles were only found on the shelf side, suggesting export into the shelf sediments, with little moving through slope waters. It is possible that internal waves could resuspend these sediments to transport this organic matter into the deep ocean (Butman et al., 2006).

The wealth of information provided by image data lends itself to the simultaneous study of many trophic levels at important physical features such as shelf-slope fronts. While images certainly have some shortcomings related to taxonomy, they can be combined with other samplers such as sediment traps, niskin bottle samples, phytoplankton sampling, and distributions of nutrients to reveal new biologically important information on fronts and other oceanographic features. Whether or not the general patterns found in this study are consistent seasonally is unknown, but the future of optical system use is promising as image acquisition, automated image analysis, and data management capabilities improve.

#### Acknowledgments

We would like to thank the captain and crew of the NOAA ship *Delaware II* for their logistical support in a successful field expedition. Jerry Prezioso and Dave Richardson helped with cruise planning, equipment setup, and shipboard plankton sample processing. Scott Sperber assisted with processing of the bongo net samples, and Dorothy Tang helped identify and count salps in the images. Mike Ford and Don Diebel

verified identifications of the hydromedusae and salps. Jean-Olivier Irlsson and Jessica Luo generously provided R code for physical data interpolation. Su Sponaugle and Peter Ortner's edits and comments substantially improved earlier versions of this work.

## References

- Aikman III, F., Ou, H.W., Houghton, R.W., 1988. Current variability across the New England continental shelf-break and slope. *Cont. Shelf Res.* 8, 625–651.
- Akima, H., Gebhardt, A., Petzoldt, T., Maechler, M., 2013. Akima: Interpolation of Irregularly Spaced Data. R Package Version 0.5-10.
- Albaina, A., Irgoien, X., 2004. Relationships between frontal structures and zooplankton communities along a cross-shelf transect in the Bay of Biscay (1995 to 2003). *Mar. Ecol. Prog. Ser.* 284, 65–75.
- Allredge, A.L., Gotschalk, C.C., 1989. Direct observations of the mass flocculation of diatom blooms: characteristics, settling velocities and formation of diatom aggregates. *Deep Sea Res. Part A* 36, 159–171.
- Allredge, A.L., Madin, L.P., 1982. Pelagic tunicates: unique herbivores in the marine plankton. *Bioscience* 32, 655–663.
- Arai, M.N., 1976. In: Mackie, G.O. (Ed.), Behavior of planktonic coelenterates in temperature and salinity discontinuity layers. *Coelenterate Ecology and Behavior*. Plenum Press, New York, pp. 211–217.
- Ashjian, C.J., Davis, C.S., Gallagher, S.M., Alatalo, P., 2001. Distribution of plankton, particles, and hydrographic features across Georges Bank described using the Video Plankton Recorder. *Deep-Sea Res.* 48, 245–282.
- Atkinson, L.P., Paffenhofer, G.A., Dunstan, W.M., 1978. Chemical and biological effect of a gulf-stream intrusion off St-Augustine, Florida. *Bull. Mar. Sci.* 28, 667–679.
- Bakun, A., 2006. Fronts and eddies as key structures in the habitat of marine fish larvae: opportunity, adaptive response and competitive advantage. *Sci. Mar.* 70, 105–122.
- Barth, J.A., Hebert, D., Dale, A.C., Ullman, D.S., 2004. Direct observations of along-isopycnal upwelling and diapycnal velocity at a shelfbreak front. *J. Phys. Oceanogr.* 34, 543–565.
- Bathmann, U.V., 1988. Mass occurrence of *Salpa fusiformis* in the spring of 1984 off Ireland: implications for sedimentation processes. *Mar. Biol.* 97, 127–135.
- Batty, R.S., 1994. The effect of temperature on the vertical distribution of larval herring (*Clupea harengus* L.). *J. Exp. Mar. Biol. Ecol.* 177, 269–276.
- Berner, L., 1967. Distributional atlas of Thaliacea in the California Current region. *CalCOFI Atlas* 8.
- Bivand, R.S., Pebesma, E.J., Gomez-Rubio, V., 2008. *Applied Spatial Analysis with R*. Springer, New York.
- Bjornsen, P.K., Nielsen, T.G., 1991. Decimeter scale heterogeneity in the plankton during a pycnocline bloom of *Gyrodinium aureolum*. *Mar. Ecol. Prog. Ser.* 73, 263–267.
- Buckley, L.J., Lough, R.G., 1987. Recent growth, biochemical composition, and prey field of larval haddock (*Melanogrammus aeglefinus*) and Atlantic cod (*Gadus morhua*) on Georges Bank. *Can. J. Fish. Aquat. Sci.* 44, 14–25.
- Buckley, L., Caldaroni, E., Ong, T., 1999. RNA–DNA ratio and other nucleic acid-based indicators for growth and condition of marine fishes. *Hydrobiologia* 401, 265–277.
- Butman, B., Alexander, P.S., Scotti, A., Beardsley, R.C., Anderson, S.P., 2006. Large internal waves in Massachusetts Bay transport sediments offshore. *Cont. Shelf Res.* 26, 2029–2049.
- Calbet, A., Saiz, E., 2005. The ciliate–copepod link in marine ecosystems. *Aquat. Microb. Ecol.* 38, 157–167.
- Cass-Calay, S.L., 2003. The feeding ecology of larval Pacific hake (*Merluccius productus*) in the California Current region: an updated approach using a combined OPC/MOCNESS to estimate prey biovolume. *Fish. Oceanogr.* 12, 34–48.
- Catalán, I.A., Vollset, K.W., Morales-Nin, B., Folkvord, A., 2011. The effect of temperature gradients and stomach fullness on the vertical distribution of larval herring in experimental columns. *J. Exp. Mar. Biol. Ecol.* 404, 26–32.
- Chapman, D.C., Lentz, S.J., 1994. Trapping of a coastal density front by the bottom boundary layer. *J. Phys. Oceanogr.* 24, 1464–1479.
- Clay, T., Bollens, S., Bochdansky, A., Ignoffo, T., 2004. The effects of thin layers on the vertical distribution of larval Pacific herring, *Clupea pallasii*. *J. Exp. Mar. Biol. Ecol.* 305, 171–189.
- Cowen, R.K., Guigand, C.M., 2008. In Situ Ichthyoplankton Imaging System (ISIS): system design and preliminary results. *Limnol. Oceanogr. Methods* 6, 126–132.
- Cowen, R.K., Greer, A.T., Guigand, C.M., Hare, J.A., Richardson, D.E., Walsh, H.J., 2013. Evaluation of the In Situ Ichthyoplankton Imaging System (ISIS): comparison with the traditional (bongo net) sampler. *Fish. Bull.* 111, 1–12.
- Davis, C.S., Flierl, G.R., Wiebe, P.H., Franks, P.J.S., 1991. Micropatchiness, turbulence and recruitment in plankton. *J. Mar. Res.* 49, 109–151.
- Davis, C.S., Gallagher, S.M., Solow, A.R., 1992. Microaggregations of oceanic plankton observed by towed video microscopy. *Science* 257, 230–232.
- Davis, C.S., Thwaites, F.T., Gallagher, S.M., Hu, Q., 2005. A three-axis fast-tow digital video plankton recorder for rapid surveys of plankton taxa and hydrography. *Limnol. Oceanogr. Methods* 3, 59–74.
- Deibel, D., 1982. Laboratory determined mortality, fecundity and growth-rates of *Thalia democratica* Forskal and *Doliolletta gegenbauri* Uljanin (Tunicata, Thaliacea). *J. Plankton Res.* 4, 143–153.
- Deibel, D., Lowen, B., 2012. A review of the life cycles and life-history adaptations of pelagic tunicates to environmental conditions. *ICES J. Mar. Sci.* 69, 358–369.
- Deibel, D., Paffenhofer, G., 2009. Predictability of patches of neritic salps and doliolids (Tunicata, Thaliacea). *J. Plankton Res.* 31, 1571–1579.
- Dekshenieks, M.M., Donaghay, P.L., Sullivan, J.M., Rines, J.E.B., Osborn, T.R., Twardowski, M.S., 2001. Temporal and spatial occurrence of thin phytoplankton layers in relation to physical processes. *Mar. Ecol. Prog. Ser.* 223, 61–71.
- Dower, J.F., Pepin, P., Leggett, W.C., 1998. Enhanced gut fullness and an apparent shift in size selectivity by radiated shanny (*Ulvaria subbifurcata*) larvae in response to increased turbulence. *Can. J. Fish. Aquat. Sci.* 55, 128–142.
- Fernández, E., Cabal, J., Acuña, J.L., Bode, A., Botas, A., García-soto, C., 1993. Plankton distribution across a slope current-induced front in the southern Bay of Biscay. *J. Plankton Res.* 15, 619–641.
- Fournier, R.O., Marra, J., Bohrer, R., Vandert, M., 1977. Plankton dynamics and nutrient enrichment of Scotian-Shelf. *J. Fish. Res. Board Can.* 34, 1004–1018.
- Fraser, J.H., 1962. Role of ctenophores and salps in zooplankton production and standing crop. Reports and Proceedings of the International Council of the Exploration of the Sea. 153, pp. 121–123.
- Gallager, S.M., Yamazaki, H., Davis, C.S., 2004. Contribution of fine-scale vertical structure and swimming behavior to formation of plankton layers on Georges Bank. *Mar. Ecol. Prog. Ser.* 267, 27–43.
- Gawarkiewicz, G., Chapman, D.C., 1992. The role of stratification in the formation and maintenance of shelf-break fronts. *J. Phys. Oceanogr.* 22, 753–772.
- Gawarkiewicz, G., Ferdelman, T.G., Church, T.M., Luther III, G.W., 1996. Shelfbreak frontal structure on the continental shelf north of Cape Hatteras. *Cont. Shelf Res.* 16, 1751–1773.
- Gawarkiewicz, G.G., Todd, R.E., Plueddemann, A.J., Andres, M., Manning, J.P., 2012. Direct interaction between the Gulf Stream and the shelfbreak south of New England. *Sci. Rep.* 2, 553.
- Genin, A., 2004. Bio-physical coupling in the formation of zooplankton and fish aggregations over abrupt topographies. *J. Mar. Syst.* 50, 3–20.
- Gordon, A., Aikman, F., 1981. Salinity maximum in the pycnocline of the Middle Atlantic Bight. *Limnol. Oceanogr.* 26, 123–130.
- Govoni, J.J., Grimes, C.B., 1992. The surface accumulation of larval fishes by hydrodynamic convergence within the Mississippi River plume front. *Cont. Shelf Res.* 12, 1265–1276.
- Graham, W.M., Pagès, F., Hamner, W.M., 2001. A physical context for gelatinous zooplankton aggregations: a review. *Hydrobiologia* 451, 199–212.
- Greer, A.T., Cowen, R.K., Guigand, C.M., McManus, M.A., Sevdjian, J.C., Timmerman, A.H.V., 2013. Relationships between phytoplankton thin layers and the fine-scale vertical distributions of two trophic levels of zooplankton. *J. Plankton Res.* 35, 939–956.
- Haddock, S.H.D., 2007. Comparative feeding behavior of planktonic ctenophores. *Integr. Comp. Biol.* 47, 847–853.
- Harbison, G., McAlister, V., Gilmer, R., 1986. The response of the salp, *Pegea confederata*, to high-levels of particulate material – starvation in the midst of plenty. *Limnol. Oceanogr.* 31, 371–382.
- Heron, A.C., 1972. Population ecology of a colonizing species: the pelagic tunicate *Thalia democratica* – I. Individual growth rate and generation time. *Oecologia* 10, 269–293.
- Hopkins, T., Lancraft, T., Torres, J., Donnelly, J., 1993. Community structure and trophic ecology of zooplankton in the Scotia Sea marginal ice-zone in winter (1988). *Deep Sea Res. Part I* 40, 81–105.
- Houde, E.D., 1989. Comparative growth, mortality, and energetics of marine fish larvae: temperature and implied latitudinal effects. *Fish. Bull.* 87, 471–495.
- Houghton, R.W., 1997. Lagrangian flow at the foot of a shelfbreak front using a dye tracer injected into the bottom boundary layer. *Geophys. Res. Lett.* 24, 2035–2038.
- Houghton, R.W., Visbeck, M., 1998. Upwelling and convergence in the Middle Atlantic Bight shelfbreak front. *Geophys. Res. Lett.* 25, 2765–2768.
- Houghton, R.W., Olson, D.B., Celone, P.J., 1986. Observation of an anticyclonic eddy near the continental shelf break south of New England. *J. Phys. Oceanogr.* 16, 60–71.
- Houghton, R.W., Aikman III, F., Ou, H.W., 1988. Shelf-slope frontal structure and cross-shelf exchange at the New England shelf-break. *Cont. Shelf Res.* 8, 687–710.
- Houghton, R.W., Vaillancourt, R.D., Marra, J., Hebert, D., Hales, B., 2009. Cross-shelf circulation and phytoplankton distribution at the summertime New England shelfbreak front. *J. Mar. Syst.* 78, 411–425.
- Jackson, G.A., 1990. A model of the formation of marine algal flocs by physical coagulation processes. *Deep Sea Res. Part A* 37, 1197–1211.
- Jacobsen, H.P., Norrbin, M.F., 2009. Fine-scale layer of hydromedusae is revealed by video plankton recorder (VPR) in a semi-enclosed bay in northern Norway. *Mar. Ecol. Prog. Ser.* 380, 129–135.
- Jossi, J.W., Marack, R.R., 1983. MARMAP plankton survey manual. U.S. Dept Com. NOAA Tech Memo., NMFS-F/NEC-21, 258 p.
- Kingsford, M.J., Suthers, I.M., 1994. Dynamic estuarine plumes and fronts: importance to small fish and plankton in coastal waters of NSW, Australia. *Cont. Shelf Res.* 14, 655–672.
- Kiorboe, T., MacKenzie, B., 1995. Turbulence-enhanced prey encounter rates in larval fish: effects of spatial scale, larval behaviour and size. *J. Plankton Res.* 17, 2319–2331.
- Kiorboe, T., Andersen, K.P., Dam, H.G., 1990. Coagulation efficiency and aggregate formation in marine phytoplankton. *Mar. Biol.* 107, 235–245.
- Kranck, K., Milligan, T.G., 1991. Grain size in oceanography. In: Syvitski, J.P.M. (Ed.), Principles, Methods, and Application of Particle Size Analysis. Cambridge University Press, Cambridge; New York, pp. 332–345.
- Landry, M.R., Ohman, M.D., Goericke, R., Stukel, M.R., Barbeau, K.A., Bundy, R., Kahru, M., 2012. Pelagic community responses to a deep-water front in the California Current Ecosystem: overview of the A-Front Study. *J. Plankton Res.* 34, 739–748.
- Leising, A.W., Pierson, J.J., Halsband-Lenk, C., Horner, R., Postel, J., 2005. Copepod grazing during spring blooms: does *Calanus pacificus* avoid harmful diatoms? *Prog. Oceanogr.* 67, 384–405.
- Linder, C.A., Gawarkiewicz, G.G., Taylor, M., 2006. Climatological estimation of environmental uncertainty over the middle Atlantic bight shelf and slope. *IEEE J. Ocean. Eng.* 31, 308–324.
- Loder, J., Drinkwater, K., Oakey, N., Home, E., 1993. Circulation, hydrographic structure and mixing at tidal fronts – the view from Georges Bank. *Philos. Trans. R. Soc. London, Ser. A* 343, 447–460.

- Lougee, L.A., Bollens, S.M., Avent, S.R., 2002. The effects of haloclines on the vertical distribution and migration of zooplankton. *J. Exp. Mar. Biol. Ecol.* 278, 111–134.
- Luo, J.Y., Grassian, B., Tang, D., Irisson, J.O., Greer, A.T., Guigand, C.M., McClatchie, S., Cowen, R.K., 2014. Environmental drivers of the fine-scale distribution of a gelatinous zooplankton community across a mesoscale front. *Mar. Ecol. Prog. Ser.* 510, 129–149.
- Malone, T.C., 1977. Plankton systematics and distribution. MESA New York Bight Atlas Monogr. 13, 0–45.
- Mann, K.H., Lazier, J.R.N., 2006. Dynamics of Marine Ecosystems: Biological–Physical Interactions in the Oceans. Blackwell, Malden, Massachusetts, USA.
- Marra, J., Houghton, R.W., Boardman, D.C., Neale, P.J., 1982. Variability in surface chlorophyll a at a shelf-break front (New York Bight). *J. Mar. Res.* 40, 575–591.
- Marra, J., Houghton, R.W., Garside, C., 1990. Phytoplankton growth at the shelf-break front in the Middle Atlantic Bight. *J. Mar. Res.* 48, 851–868.
- McClatchie, S., Cowen, R., Nieto, K., Greer, A., Luo, J.Y., Guigand, C., Demer, D., Griffith, D., Rudnick, D., 2012. Resolution of fine biological structure including small narcomedusae across a front in the Southern California Bight. *J. Geophys. Res. C Oceans* 117.
- McManus, M.A., Cheriton, O.M., Drake, P.J., Holliday, D.V., Storlazzi, C.D., Donaghay, P.L., Greenlaw, C.F., 2005. Effects of physical processes on structure and transport of thin zooplankton layers in the coastal ocean. *Mar. Ecol. Prog. Ser.* 301, 199–215.
- Miller, T.J., 2002. Assemblages, communities, and species interactions. In: Fuiman, L.A., Werner, R.G. (Eds.), *Fishery Science: The Unique Contributions of the Early Life Stages*. Blackwell Science Ltd, pp. 183–205.
- Mills, C.E., 1984. Density is altered in hydromedusae and ctenophores in response to changes in salinity. *Biol. Bull.* 166, 206–215.
- Miralto, A., Barone, G., Romano, G., Poulet, S.A., Ianora, A., Russo, G.L., Buttino, I., Mazzarella, G., Laabir, M., Cabrini, M., Glacobbe, M.G., 1999. The insidious effect of diatoms on copepod reproduction. *Nature* 402, 173–176.
- Morote, E., Olivar, M.P., Bozzano, A., Villate, F., Uriarte, I., 2011. Feeding selectivity in larvae of the European hake (*Merluccius merluccius*) in relation to ontogeny and visual capabilities. *Mar. Biol.* 158, 1349–1361.
- Mountain, D., 2003. Variability in the properties of shelf water in the Middle Atlantic Bight, 1977–1999. *J. Geophys. Res. Oceans* 108, 3014.
- Munk, P., 2014. Fish larvae at fronts: horizontal and vertical distributions of gadoid fish larvae across a frontal zone at the Norwegian Trench. *Deep-Sea Res. II Top. Stud. Oceanogr.* 107, 3–14.
- Munk, P., Hansen, B.W., Nielsen, T.G., Thomsen, H.A., 2003. Changes in plankton and fish larvae communities across hydrographic fronts off West Greenland. *J. Plankton Res.* 25, 815–830.
- Nielsen, T.G., Munk, P., 1998. Zooplankton diversity and the predatory impact by larval and small juvenile fish at the Fisher Banks in the North Sea. *J. Plankton Res.* 20, 2313–2332.
- Norrbin, M.F., Vis, C.S.D.A., Gallagher, S.M., 1996. Differences in fine-scale structure and composition of zooplankton between mixed and stratified regions of Georges Bank. *Deep-Sea Res. II* 43, 1905–1924.
- Oksanen, J., Blanchet, F.G., Kindt, R., Legendre, P., Minchin, P.R., O'Hara, R.B., Simpson, G.L., Solymos, P., Stevens, M.H.H., Wagner, H., 2013. *vegan: Community Ecology Package*. Paffenhöfer, G., Lee, T.N., 1987. Development and persistence of patches of *Thalassia*. *S. Afr. J. Mar. Sci.* 5, 305–318.
- Paffenhöfer, G.A., Atkinson, L.P., Lee, T.N., Verity, P.G., Bulluck, L.R.I.I., 1995. Distribution and abundance of thalassians and copepods off the southeastern USA during winter. *Cont. Shelf Res.* 15, 255–280.
- Pebesma, E.J., 2004. Multivariate geostatistics in S: the gstat packages. *Comput. Geosci.* 30, 683–691.
- Pebesma, E.J., Bivand, R., 2005. S classes and methods for spatial data in R. *R News* 5.
- Pepin, P., 1991. Effect of temperature and size on development, mortality, and survival rates of the pelagic early life history stages of marine fish. *Can. J. Fish. Aquat. Sci.* 48, 503–518.
- Pierson, J.J., Leising, A.W., Halsband-Lenk, C., Ferm, N., 2005. Vertical distribution and abundance of *Calanus pacificus* and *Pseudocalanus newmani* in relation to chlorophyll a concentrations in Dabob Bay, Washington. *Prog. Oceanogr.* 67, 349–365.
- R Core Team, 2013. R: A Language and Environment for Statistical Computing. <http://www.R-project.org>.
- Rasband, W.S., 1997–2012. ImageJ. U.S.
- Reeve, M.R., Walter, M.A., Ikeda, T., 1978. Laboratory studies of ingestion and food utilization in lobate and tentaculate ctenophores. *Limnol. Oceanogr.* 23, 740–751.
- Remsen, A., Hopkins, T.L., Samson, S., 2004. What you see is not what you catch: a comparison of concurrently collected net, Optical Plankton Counter, and Shadowed Image Particle Profiling Evaluation Recorder data from the northeast Gulf of Mexico. *Deep-Sea Res. I Oceanogr. Res. Pap.* 51, 129–151.
- Rothschild, B.J., Osborn, T.R., 1988. Small-scale turbulence and plankton contact rates. *J. Plankton Res.* 10, 465–474.
- Sabatés, A., Pages, F., Atienza, D., Fuentes, V., Purcell, J.E., Gili, J., 2010. Planktonic cnidarian distribution and feeding of *Pelagia noctiluca* in the NW Mediterranean Sea. *Hydrobiologia* 645, 153–165.
- Sheldon, R.W., Prakash, A., Sutcliffe, W.H., 1972. The size distribution of particles in the ocean. *Limnol. Oceanogr.* 17, 327–340.
- Steele, J.H., 1978. Spatial Pattern in Plankton Communities. p. 470.
- Stemmman, L., Boss, E., 2012. Plankton and particle size and packaging: from determining optical properties to driving the biological pump. *Ann. Rev. Mar. Sci.* 4, 263–290.
- Sumida, B.Y., Moser, H.G., 1980. Food and feeding of Pacific hake larvae, *Merluccius productus*, off southern California and northern Baja California. *Calif. Coop. Ocean. Fish. Investig. Rep.* 21, 161–166.
- Titelman, J., Hansson, L.J., Nilsen, T., Colin, S.P., Costello, J.H., 2012. Predator-induced vertical behavior of a ctenophore. *Hydrobiologia* 690, 181–187.
- Tosti, E., Romano, G., Buttino, I., Cuomo, A., Ianora, A., Miralto, A., 2003. Bioactive aldehydes from diatoms block the fertilization current in ascidian oocytes. *Mol. Reprod. Dev.* 66, 72–80.
- Toyokawa, M., Toda, T., Kikuchi, T., Miyake, H., Hashimoto, J., 2003. Direct observations of a dense occurrence of *Bolinopsis infundibulum* (Ctenophora) near the seafloor under the Oyashio and notes on their feeding behavior. *Deep Sea Res. Part I* 50, 809–813.
- Tsuda, A., Nemoto, T., 1992. Distribution and growth of salps in a Kuroshio warm-core ring during summer 1987. *Deep Sea Res. Part A* 39, S219–S229.
- Vlymen, W.J., 1977. A mathematical model of the relationship between larval anchovy (*Engraulis mordax*) growth, prey microdistribution, and larval behavior. *Environ. Biol. Fish.* 2, 211–233.
- Woodson, C.B., Webster, D.R., Weissburg, M.J., Yen, J., 2005. Response of copepods to physical gradients associated with structure in the ocean. *Limnol. Oceanogr.* 50, 1552–1564.
- Woodson, C.B., Webster, D.R., Weissburg, M.J., Yen, J., 2007. Cue hierarchy and foraging in calanoid copepods: ecological implications of oceanographic structure. *Mar. Ecol. Prog. Ser.* 330, 163–177.
- Woodward, G., Ebenman, B., Emmerson, M., Montoya, J.M., Olesen, J.M., Valido, A., Warren, P.H., 2005. Body size in ecological networks. *Trends Ecol. Evol.* 20, 402–409.
- Zhang, W.G., McGillicuddy Jr., D.J., Gawarkiewicz, G.G., 2013. Is biological productivity enhanced at the New England shelfbreak front? *J. Geophys. Res. C Oceans* 118, 517–535.